International Journal of Electrical, Electronic and Communication Sciences
ISSN: 2517-9438
Vol:6, No:12, 2012

# Thermal Analysis of the Current Path from Circuit Breakers Using Finite Element Method

Adrian T. Plesca

***Abstract*—**This paper describes a three-dimensional thermal model of the current path included in the low voltage power circuit breakers. The model can be used to analyse the thermal behaviour of the current path during both steady-state and transient conditions. The current path lengthwise temperature distribution and time-current characteristic of the terminal connections of the power circuit breaker have been obtained. The influence of the electric current and voltage drop on main electric contact of the circuit breaker has been investigated. To validate the three-dimensional thermal model, some experimental tests have been done. There is a good correlation between experimental and simulation results.

***Keywords*—**Current path, power circuit breakers, temperature distribution, thermal analysis.

## I. Introduction

CIRCUIT breakers are designed to switch a wide range of currents. They not only have to provide over current and short-circuit current protection, but must switch load current and isolate sections of the low-voltage distribution system. A typical circuit breaker in service will be conducting current when the system is energized. In this mode, the contacts are closed and a continuous current goes through the breaker. It results a Joule heating of the current conducting components, such as the contacts, the trip units, fixed parts of the current path and the flexible connections. The breaker therefore has to dissipate effectively the heat that is generated within it by these components. The conducting components that change most with usage are the contacts. There are Underwriters' Laboratories (UL) Standard tests for molded-case circuit breakers which include temperature-rise measurements at the circuit breaker terminals while carrying rated current after the circuit breaker has interrupted an overload current (600% of rated current) 50 times. Therefore, the temperature variation provides important information about early hidden troubles of power circuit breakers and becomes a significant parameter in order to monitor and diagnose different types of circuit breakers. In previous works, analytical procedures aimed to identify different perturbation sources in the diagnostic of power equipment and structures that may be exposed to a variety of upsetting phenomena are presented in [1]. The automated circuit breaker diagnostic system described in [2], is an extension of the widely used portable circuit breaker testing device concept and an overview is given in [3], [4] on diagnosis techniques for the circuit breaker technical state valuation. Certification tests in accordance with the requirements of the IEC 61259 standard for switching of bus-charging current by disconnectors of a three-phase enclosed gas insulated switchgear are presented in [5]. Combined analytical simulations have been performed in [6] for analyzing and optimizing the behaviour of low-voltage circuit-breakers. In [7] a method is proposed, concerning the temperature rise estimation at stationary electrical contacts, operating in the power supply network, during short-circuit. A theoretical and experimental investigation was attempted of the mechanisms that can affect heat transfer to a component-conductor system in [8] and new materials to be used at electric contacts are presented in [9]. The interrelation of gas dynamic and magnetic forces is investigated by developing relationships between electromagnetic forces and high temperature gas dynamic flows [10]-[12]. Besides electrical contacts, important components for power circuit breakers are represented by its main current path and busbars. There are many previous papers which have studied the busbar technology from mechanical or thermal point of view, such as analysis of electromagnetic and thermal fields [13] or temperature distribution over the surface of busbars [14]. The long-term reliability of busbars and the integrity of insulating materials have been studied in [15]-[17]. A mathematical model is proposed in [18] for the steady-state temperature difference distribution of double-break DC contactors.

This study attempts to develop a three-dimensional thermal model of main current path of a molded-case circuit breaker, for both steady-state and transient operating conditions.

A. T. Plesca is with the Gheorghe Asachi Technical University of Iasi, Iasi, IS 700050 Romania (phone: 40-232-278683; fax: 40-232-237627; e-mail: aplesca@ee.tuiasi.ro).

## II. Thermal Model

The balance equation of heat transfer for the main current path of the power circuit breaker has the following expression,

$$Q_t = Q_r + Q_c - Q_a \tag{1}$$

The left term of the equation means the heat stored by temporal change of temperature $Q_t$. It is in balance with the heat removed from the current path by thermal conduction $Q_r$, the heating power from the current flow, $Q_c$ and the thermal power dissipated to the surrounding area by the surface convection, $Q_a$. For $Q_c$, $Q_t$, $Q_r$ and $Q_a$, the following equations can be written:

$$Q_t = \gamma c \frac{\partial \theta}{\partial t} \tag{2}$$

$$Q_r = div(\lambda grad\theta) \tag{3}$$

$$Q_c = \rho j^2 \tag{4}$$

$$Q_a = k\frac{l_p}{S}(\theta - \theta_a) \tag{5}$$

where j means current density; ρ – electrical resistivity; γ – material density; c – specific heat; λ – thermal conductivity; θ – temperature; k - convection coefficient. Therefore,

$$\gamma c\frac{\partial\theta}{\partial t} = div(\lambda grad\theta) + \rho j^2 - k\frac{l_p}{S}(\theta - \theta_a) \tag{6}$$

The current path from the power circuit breaker has variable cross-section S = S(x,y,z) and thus, variable perimeter length $l_p = l_p(x,y,z)$ of the cross-section. The electrical resistivity has a significant temperature variation and can be estimated through a linear one,

$$\rho = \rho_0[1 + \alpha(\theta - \theta_a)] \tag{7}$$

and with the notations:

$$\vartheta = \theta - \theta_a; \quad j = \frac{I}{S} \tag{8}$$

the following relation is obtained:

$$\frac{\gamma c}{\lambda}\frac{\partial\vartheta}{\partial t} = \frac{\partial^2\vartheta}{\partial x^2} + \frac{\partial^2\vartheta}{\partial y^2} + \frac{\partial^2\vartheta}{\partial z^2} + \left(\frac{\rho_0\alpha I^2}{\lambda S(x,y,z)^2} - \frac{l_p(x,y,z)k}{\lambda S(x,y,z)}\right)\vartheta + \frac{\rho_0 I^2}{\lambda S(x,y,z)^2} \tag{9}$$

The above expression is complex, and it demands a numerical procedure to evaluate the temperature distribution both in steady-state or transient conditions. It is desirable to restate the problem by considering various forms of discretization. The discretized form of the problem only requires the solution to be satisfied at a finite number of points in the region; in the remaining of the region, appropriate interpolations may be used. Thus, this case is reduced to a purely algebraic form involving only the basic arithmetic operations, which could in turn be solved by numerical methods. Using Galerkin method and including convection boundary condition, the discretized equations for the heat transfer are as follows:

$$\int_V \gamma c\frac{\partial\theta}{\partial t}N_i dV + \int_V \left[\frac{\partial N_i}{\partial x}\ \frac{\partial N_i}{\partial y}\ \frac{\partial N_i}{\partial z}\right]\lambda[B]\{\theta\}dV = \int_V \rho j^2 N_i dV - \int_S k(\theta - \theta_a)N_i dS \tag{10}$$

where [N] is the matrix of shape functions and [B] is the matrix for temperature gradients interpolation. Shape functions $N_i$ are used for interpolation of temperature and temperature gradients inside a finite element:

$$\theta = [N]\{\theta\}, \quad [N] = [N_1\ N_2\ N_3 \ldots], \quad \{\theta\} = \{\theta_1\ \theta_2\ \theta_3 \ldots\}$$
$$\begin{Bmatrix}\frac{\partial\theta}{\partial x}\\ \frac{\partial\theta}{\partial y}\\ \frac{\partial\theta}{\partial z}\end{Bmatrix} = \begin{bmatrix}\frac{\partial N_1}{\partial x} & \frac{\partial N_2}{\partial x} & \frac{\partial N_3}{\partial x}\ldots\\ \frac{\partial N_1}{\partial y} & \frac{\partial N_2}{\partial y} & \frac{\partial N_3}{\partial y}\ldots\\ \frac{\partial N_1}{\partial z} & \frac{\partial N_2}{\partial z} & \frac{\partial N_3}{\partial z}\ldots\end{bmatrix}\{\theta\} = [B]\{\theta\} \tag{11}$$

The finite element equations corresponding to the heat transfer, have the following matrix form:

$$[A]\{\dot{\theta}\} + ([L_c] + [L_k])\{\theta\} = \{R_Q\} + \{R_k\} \tag{12}$$

$$[A] = \int_V [N]^T \gamma c[N]dV; \quad [L_c] = \int_V [B]^T \lambda[B]dV; \quad [L_k] = \int_S [N]^T k[N]dS \tag{13}$$

$$[R_Q] = \int_V \rho j^2 [N]^T dV; \quad [R_k] = \int_S k\theta_a [N]^T dS \tag{14}$$

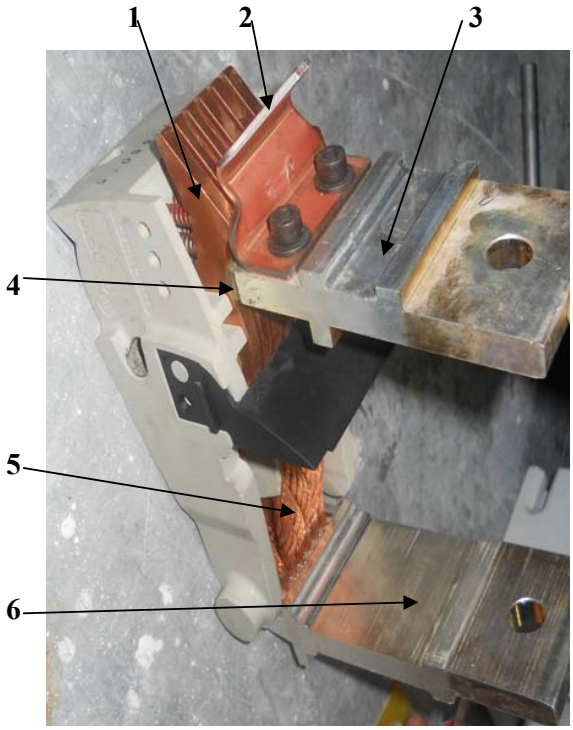


Fig. 1 Main component parts of the current path of the power circuit breaker (1 – breaking movable contact; 2 – breaking fixed contact; 3 – top current path; 4 – electric contact; 5 – flexible current path; 6 – bottom current path)

A 3D model for the main current path from a power circuit breaker has been developed using specific software, the Pro-ENGINEER, an integrated thermal design tool for all type of accurate thermal analysis on devices. The subject was a

molded case circuit breaker type IZMB1-V1000 with rated current by 1000A, rated frequency of 50Hz and rated operational voltage by 440V/690V according to a rated service short-circuit breaking capacity of 50kA/42kA. The main component parts for a single-pole current path are outlined in Fig. 1. The 3D model takes into consideration all the component parts of main current path, including the shaft and joining pieces for flexible current path with the aim to connect it with breaking fixed contact and bottom current path, as shown in Fig. 2. It was considered a simplified geometry for the screws. The flexible current path is made from 12 beams of thin twisted copper wires mounted in parallel, through joining pieces, between bottom current path and breaking movable contact. The flexible current path has been modelled using 12 copper cylinders taking into account the equivalent thermal resistance.

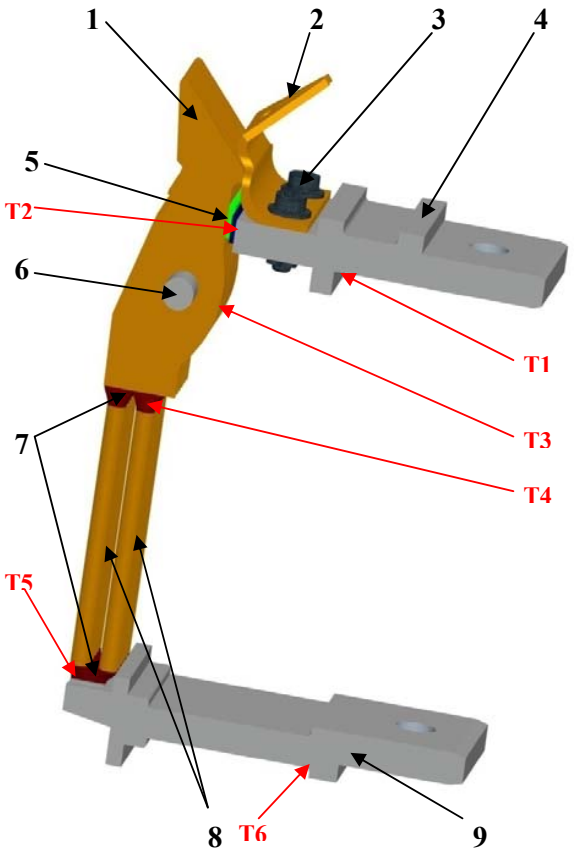


Fig. 2 Current path thermal model (1 – breaking movable contact; 2 – breaking fixed contact; 3 – screw; 4 - top current path; 5 – electric contact; 6 – shaft; 7 – joining pieces; 8 - flexible current path; 9 – bottom current path) and the temperature measurement points (T1…T6)

The main or current-carrying copper contacts are typically of the butt type with silver facings for the lower currents. The multiple-finger type for the higher current ratings is faced with silver-tungsten.

## III. Thermal Simulations

A typical application is when this type of circuit breaker is used to protect against over loads and short-circuits a low voltage power distribution system. The current which flows through the circuit breaker current path has been considered about 1000A, the rated one. At this current value, some experimental tests have been done in order to estimate the voltage drop across different component parts of the main current path, and then to compute the partial power losses, actually the heat load. Therefore, after measurements and calculations, the following power loss values have been obtained: 17W on the top current path, 27W across the main electric contact, 15W on the breaking movable contact, 22W across flexible current path, 20W on the bottom current path and about 7W in joining pieces placed on the terminals of the flexible current path.

For all thermal simulations 3D finite elements Pro-MECHANICA software has been used. The material properties of every component part of the single-pole current path are described in the Table I, according to Fig. 2. The heat load has been applied on every main component parts of the current path. There is a uniform spatial distribution on every component.

TABLE I
Material Data and Coefficients at 20°C according with the Component Parts from Fig. 2

| Parameter | Material | | |
|---|---|---|---|
| | Copper (1, 2, 4, 7, 8, 9) | Iron FE40 (3, 6) | Silver-Tungsten (5) |
| γ [kg/m$^3$] | 8920 | 7860 | 14900 |
| c [J/kg°C] | 385 | 25.10 | 186 |
| λ [W/m°C] | 401 | 52 | 289 |

The mesh of this 3D current path thermal model has been done using tetrahedron solids element types. The single pass adaptive convergence method to solve the thermal steady-state simulation has been used. The cross-section of both top and bottom current path is 55mm x 10mm. The ambient temperature was about 25ºC and inside the molded case where the current path is mounted, a temperature of 32 ºC has been measured.

From experimental tests, it was computed k = 19.5W/m$^2$ºC, for this type of current path. Hence, it was considered the convection condition like boundary condition for the outer boundaries as breaking movable contact, breaking fixed contact, top current path, electric contact, flexible current path, shaft, joining pieces and bottom current path, and it has been applied on surfaces with a uniform spatial variation and a bulk temperature of 25ºC. In the case of the components of the current path placed inside the molded-case, a bulk temperature of 32ºC has been considered.

Further on, some steady state thermal simulations have been done. The temperature distribution inside the current path is shown in Fig. 3.

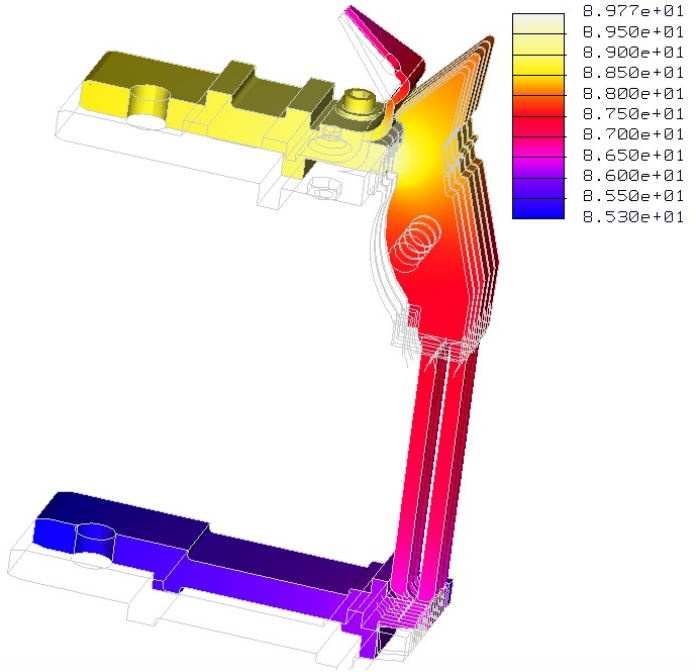


Fig. 3 Temperature distribution through the current path (50% cross-section)

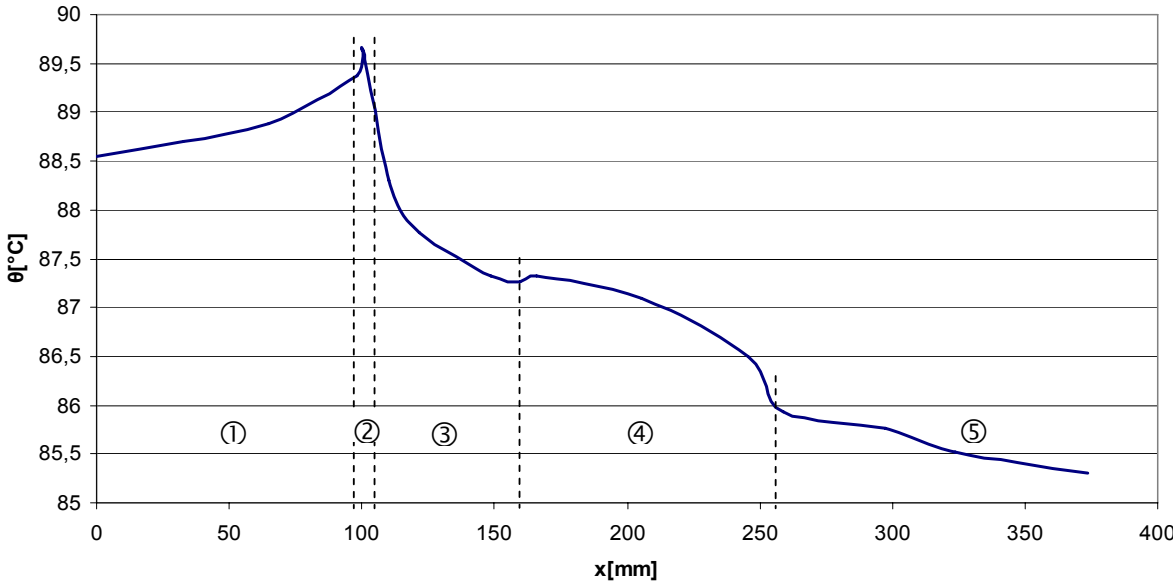


Fig. 4 Temperature distribution lengthwise the current path at rated current of 1000A. The outlined areas mean: 1 – top fixed current path; 2 – main contact; 3 – movable contact; 4 – flexible connection; 5 – bottom fixed current path

The current path lengthwise temperature distribution is presented in Fig. 4. The same current path lengthwise temperature distribution but at different contact voltage drops, is shown in Fig. 5.

In order to analyse the time evolution of the temperature for the current path, a series of transient thermal simulations have been done.

The measure points T1…T6, are marked in the Fig. 2. The temperature evolutions of the main electric contact of the current path, actually the hot spot temperature, and temperature variations of the top and bottom current path, are presented in Fig. 6. The main contact temperature time evolution at different current values and different voltage drops are depicted in the graphics from Fig. 7 and Fig. 8.

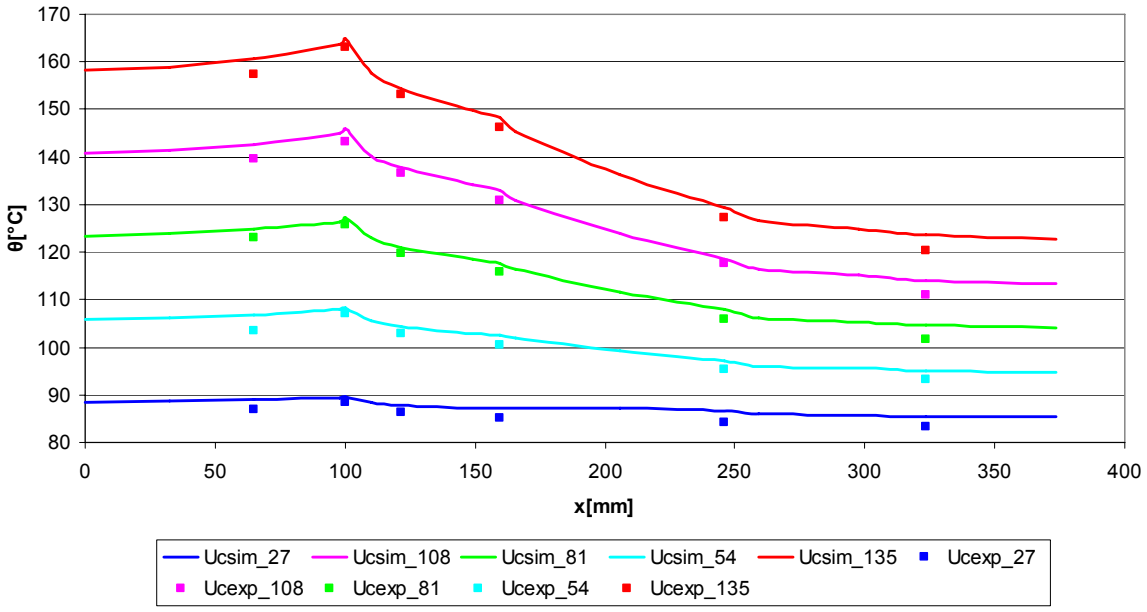


Fig. 5 Temperature distribution lengthwise the current path at rated current of 1000A and different main contact voltage drop (27, 54, 81, 108 and 135mV). Comparison between simulation results (Ucsim_27, Ucsim_54, Ucsim_81, Ucsim_108, Ucsim_135) and experimental values (Ucexp_27, Ucexp_54, Ucexp_81, Ucexp_108, Ucexp_135)

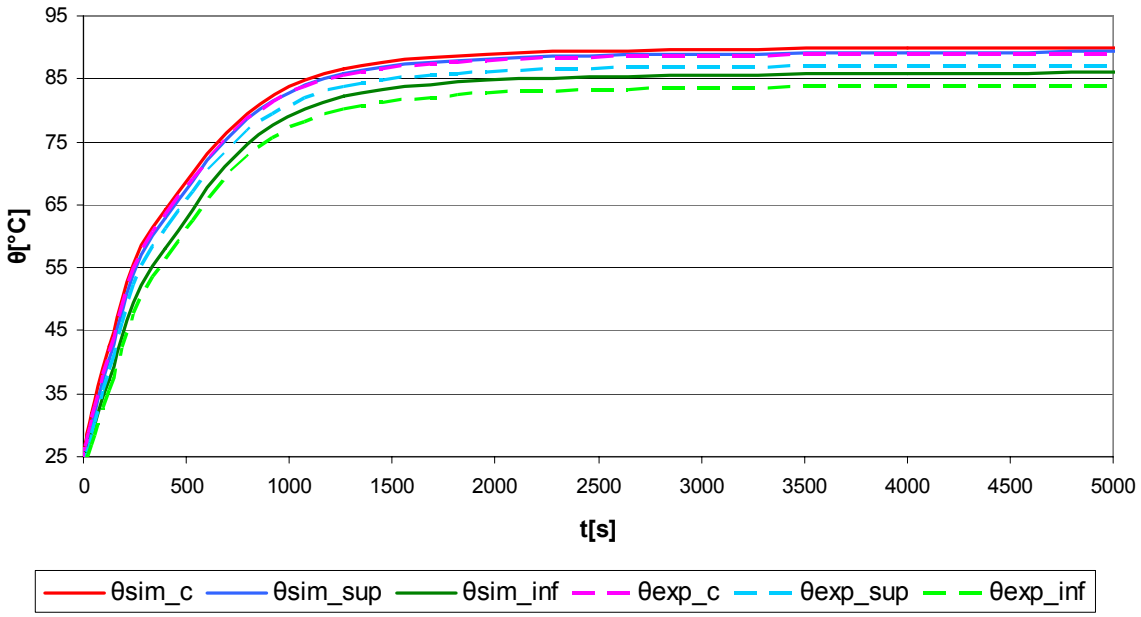


Fig. 6 Temperature variation of the current path at rated current of 1000A for main contact, top fixed current path and bottom fixed current path. Comparison between simulation results (θsim_c, θsim_sup, θsim_inf) and experimental values (θexp_c, θexp_sup, θexp_inf)

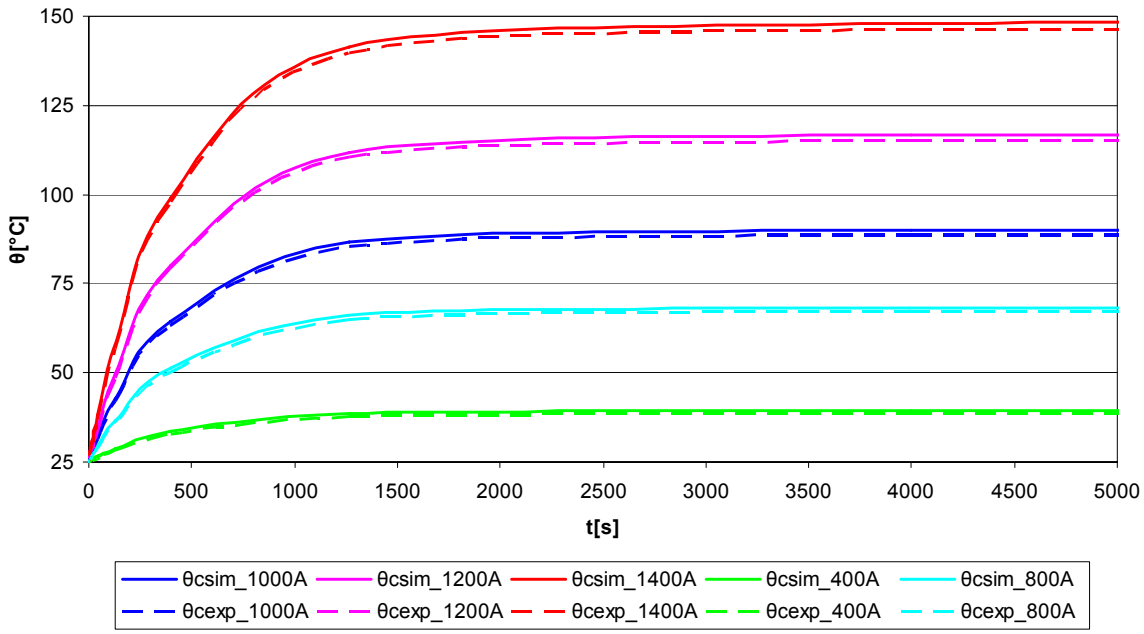


Fig. 7 Temperature variation of the main contact from the current path at different current values (400, 800, 1000, 1200 and 1400A). Comparison between simulation results (θcsim_400A, θcsim_800A, θcsim_1000A, θcsim_1200A, θcsim_1400A) and experimental values (θcexp_400A, θcexp_800A, θcexp_1000A, θcexp_1200A, θcexp_1400A)

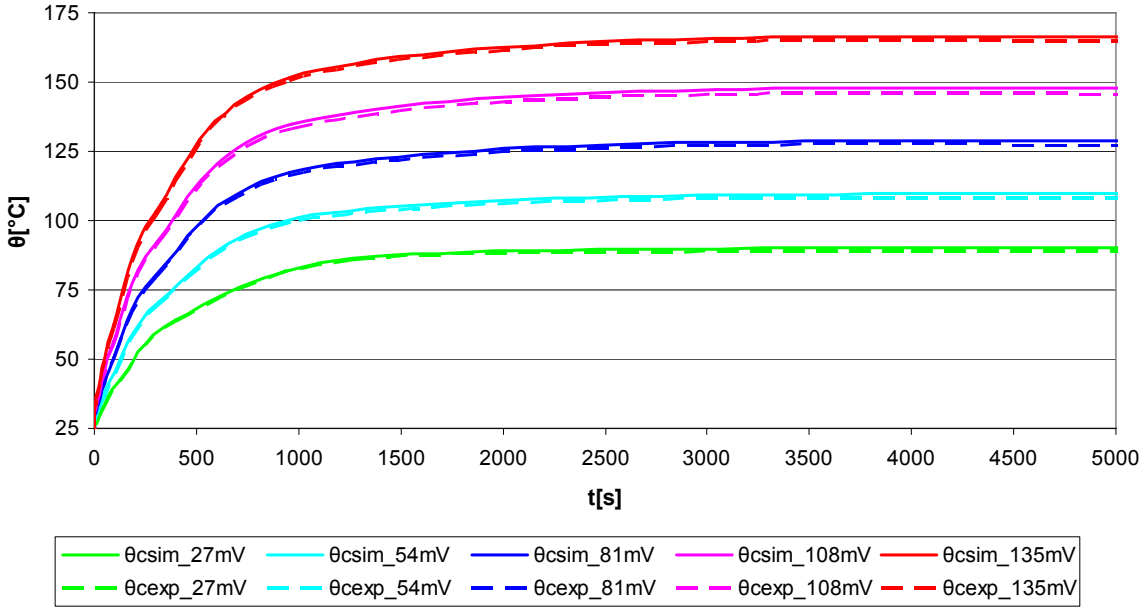


Fig. 8 Temperature variation of the main contact from the current path at different drop voltage values (27, 54, 81, 108 and 135mV). Comparison between simulation results (θcsim_27mV, θcsim_54mV, θcsim_81mV, θcsim_108mV, θcsim_135mV) and experimental values (θcexp_27mV, θcexp_54mV, θcexp_81mV, θcexp_108mV, θcexp_135mV)

## IV. Discussion of the Results

As can be seen in the 3D thermal simulation picture from Fig. 3, and the current path lengthwise temperature distribution from Fig. 4, the maximum temperature (89.77°C) is obtained in the main electric contact (area 2 on Fig. 4). This is explained because of power loss (27W) generated at the contact, due to the contact resistance during current conduction. This is the highest power loss value respect to the other component parts of the circuit breaker current path. The minimum temperature (85.3°C) belongs to the bottom current path (area 5 on Fig. 4) at the end terminal connection. On the other hand, there is not a big difference between maximum and minimum temperature, only 4.47°C. High temperature values can be noticed on the top current path (area 1 on Fig. 4), around 89°C, which can be explained because of the short distance respect to the main electric contact which has the maximum temperature. The current path lengthwise temperature distribution at different voltage drop values (27, 54, 81, 108 and 135mV) on main electric contact is presented in Fig. 5. As expected, at higher voltage drops, higher maximum temperatures are obtained. The highest value of the maximum temperature (164.79°C) corresponds to the case when the voltage drop has the value of 135mV. The thermal simulations have been done for the rated current of 1000A and the ambient temperature of 25°C. Also, at higher voltage drop values, the difference between minimum and maximum temperature is increased. Thus, at 27mV voltage drop on main contact, the difference is 4.47°C, and in the case with 135mV, the difference between extreme temperatures is about 42°C, almost 10 times than normal operating conditions for the circuit breaker.

The time temperature evolution of the current path for normal operating conditions of the circuit breaker (rated current of 1000A, voltage drop on main electric contact of 27mV and ambient temperature of 25°C) is presented in Fig. 6. Because the difference between maximum and minimum temperature is only 4.47°C, the graphics show the temperature evolution only for main contact (θsim_c), top current path (θsim_sup) and bottom current path (θsim_inf), according to the measurement points T2, T1 and T6 from Fig. 2. It is to observe that steady-state conditions are fulfilled after approximately two hours with the following temperature values: 89.77°C for main contact, 88.89°C at top current path and 85.52°C in the bottom current path. Because the maximum temperature belongs to the contact between fixed and movable component parts of the current path, the next transient thermal simulations will take into consideration only this temperature.

The time temperature evolution of the main contact at different current values is presented in Fig. 7. As expected, at higher current value, higher temperatures are obtained. Starting from the minimum adjusted current of 400A, which can be obtained with the analysed circuit breaker IZMB1-V1000, the transient thermal simulations have been performed up to the overload value of 1400A. The steady-state temperatures starts from 39.29°C (θcsim_400A) and goes up to 147.16°C (θcsim_1400A).

Aiming to analyse the time temperature evolution at different voltage drops, the same values have been considered as in the case of steady-state thermal simulations. The graphics are shown in Fig. 8. It is to notice the temperature increasing from 89.77°C (θcsim_27mV) up to 164.79°C (θcsim_135mV), according to a voltage drop increasing from 27mV to 135mV. For all transient simulations, the current value was the same, 1000A.

According to the standard IEC 60947-2, the temperature rise of the circuit breaker terminals for external connections, is limited to 80°C. At an ambient temperature of 25°C, results an admissible temperature of 105°C for the terminals, actually, the top and bottom current path of the circuit breaker. Thus, it is important to analyse the temperature evolution of the circuit breaker terminals at different over currents. When the over current increases, the time of the temperature evolution from ambient value to the admissible one will decrease. Finally, results a time-current characteristic for the external connections of the circuit breaker current path. Because the higher temperatures belong to the top side of the current path, the temperature in the point T1 has been computed at different prospective currents, during transient thermal simulations, Fig. 2. The comparison between time-current characteristic of the current path terminals, θlim, and protection characteristics of the power circuit breaker at minimum setting, IZMB1min, and maximum setting, IZMB1max, is depicted in Fig. 9. It is to observe that both protection characteristics are below time-current characteristic of the terminals. This means the external connections of the current path are protected from thermal point of view in both situations when the circuit breaker has minimum or maximum settings for its protection characteristics.

To validate the thermal model some experimental tests have been made in the same conditions as in the case of thermal simulations. An electric circuit diagram used for experimental tests is shown in Fig. 10.

The main switch K allows to supply the auto-transformer ATR, which adjusts the input voltage for the high current supply device CS. This has an adjustable primary voltage and on the secondary side, high value current can be obtained. The current value is measured by an ammeter A through a current transformer CT. Using proper thermocouples Th, type K, the temperatures from the same measurement points (T1…T6) as in the thermal simulations Fig. 2, have been acquired. The small voltage signals provided by thermocouples have been amplified using a signal conditioning board type AT2F-16 with the error of ± 0.5%. The amplified signal was the input for a data acquisition board type PC-LPM-16 which can be programmed with LabVIEW software. The sampling rate was 50kS/s and the analogue inputs have a resolution on 12 bits. The comparisons between simulation and experimental results are presented from Fig. 5 to Fig. 8. The experimental temperature values are smaller than the simulation ones. This is because during the experimental tests there are busbars to connect the power circuit breaker with protected electrical installations. Because of their volume and thermal capacity, all these components act like real heatsinks for the circuit breaker, leading to an important heat dissipation rate.

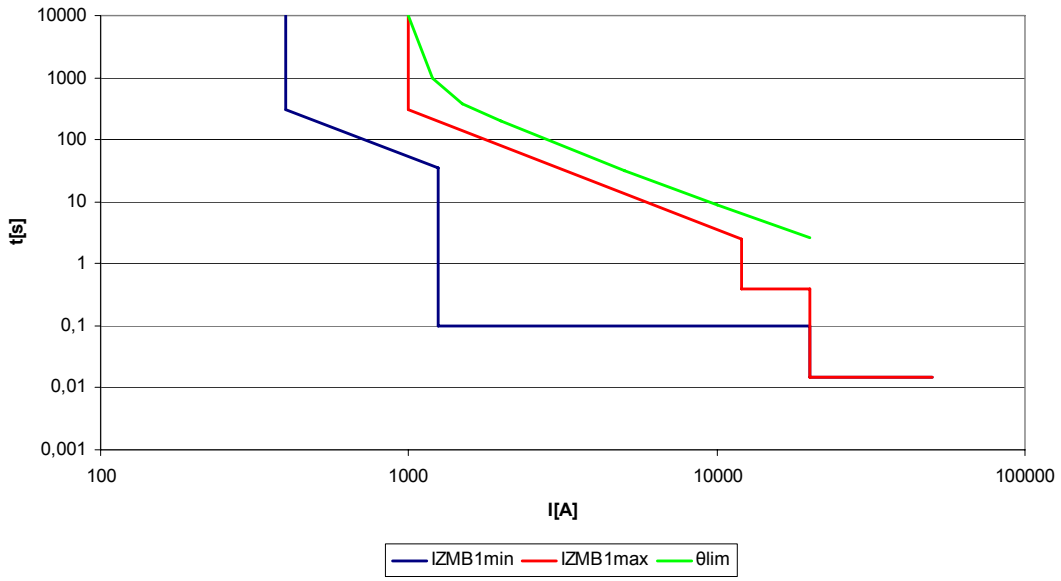


Fig. 9 Comparison between time-current characteristic of the current path (θlim) and protection characteristics of the circuit breaker with minimum adjusting (IZMB1min) and maximum adjusting (IZMB1max)

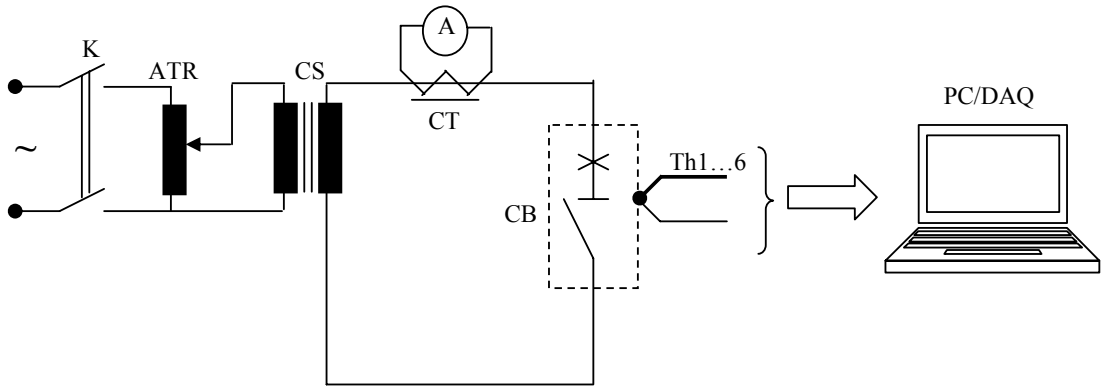


Fig. 10 Experimental main circuit

On the other hand, the differences between the temperature values resulting from experimental tests and those obtained during simulations are due to various factors: measurement errors, thermal model simplifications and mounting test conditions. The thermal model has not included different types of current busbars from the circuit breaker terminal connections to different electrical devices to be protected. Nevertheless, the maximum difference between the experimental and simulation results is less than 3.5ºC.

## V. Conclusion

To understand and to optimize the operating mechanisms of power circuit breakers, the thermal behaviour of the current path is of great interest. The obtained 3D thermal model allows analysis of the thermal behaviour of current paths from power circuit breakers during both steady-state or transient conditions.

The thermal model provides the current path lengthwise temperature distribution, the time-current characteristic of the external connections of the current path and could be used as a tool for different types of low voltage power circuit breaker designing. Some experimental tests have been made with the aim to validate the proposed 3D thermal model. The maximum difference between the experimental and simulation results is less than 3.5°C. Using the proposed 3D thermal model the circuit breaker designing can be improved and there is the possibility to obtain new solutions for a better correlation between protection characteristics of the switchgears and their terminal connections, as busbars, from power electrical installations.

## Acknowledgment

This work was supported by CNCSIS – UEFISCDI, project number 515 PNII – CAPACITATI, 2011.

## REFERENCES

[1] C. Bartoletti, G. Fazio, F. Muzi, S. Ricci, and G. Sacerdoti, "Diagnostics of electric power components: An improvement on signal discrimination," *WSEAS Trans. on Circuits and Systems*, vol. 4, pp. 788-795, 2005.

[2] M. Kezunovic, C. Nail, Z. Ren, D. R. Sevcik, J. Lucey, W. Cook, and E. Koch, "Automated circuit breaker monitoring and analysis," in *Proc. of the IEEE Power Engineering Society Transmission and Distribution Conf.*, 2002, pp. 559-564.

[3] I. Manea, C. Chiciu, F. Balasiu, and N. Tulici, "Complex methods to diagnose the technical state of the medium and high voltage circuit breaker after short-circuit events," in *2001 IEE Conf. Publication 1* pp. 482.

[4] M. Adam, A. Baraboi, C. Pancu, and A. Plesca, "Reliability centered maintenance of the circuit breakers," *International Review of Electrical Engineering*, vol. 5, pp. 1218-1224, 2010.

[5] R. P. Smeets, Van Der Linden, W. A., Achterkamp, M., Damstra, and E. M. De Meulemeester, "Disconnector switching in GIS: three-phase testing and phenomena," *IEEE Trans. on Power Delivery*, vol. 15, pp. 122-127, 2000.

[6] T. Mutzel, F. Berger, and M. Anheuser, "Numerical analysis of low-voltage circuit-breakers under short-circuit conditions," in *The 53rd IEEE Holm Conf. on Electrical Contacts*, 2007, pp. 37 – 42.

[7] M. P. Filippakou, C. G. Karagiannopoulos, D. P. Agoris, and P. D. Bourkas, "Electrical contact overheating under short-circuit currents," *Electric Power Systems Research*, vol. 57, pp. 141-147, 2001.

[8] C. G. Aronis, C. G. Karagiannopoulos, P. D. Bourkas, and N. J. Theodorou, "Dimensioning components installed in electrical panels with respect to operational temperature," *IEE Proc. - Science Measurement and Technology*, vol. 152, pp. 36 – 42, 2005.

[9] L. G. Bujoreanu, "On the influence of austenitization on the morphology of α-phase in tempered Cu–Zn–Al shape memory alloys," *Materials Science and Engineering A* vol. 481–482, pp. 395–403, 2008.

[10] N. Du, Y. Guan, W. Liu, S. Jin, and M. Collod, "Current distribution and thermal effects analysis on the sliding contact arrangement in circuit breaker," in *International Conf. on Electrical Machines and Systems*, 2008, pp. 447 – 451.

[11] N. P. Basse, M. Seeger, C. M. Franck, and T. Votteler, "Thermal interruption performance and fluctuations in high voltage gas circuit breakers," in *The 33rd IEEE International Conf. on Plasma Science*, 2006, pp. 86.

[12] K. Pechrach, J. W. McBride, and P. M. Weaver, "The correlation of magnetic, gas dynamic and thermal effects on arc mobility in low contact velocity circuit breakers," in *Proc. of the Forty-Eighth IEEE Holm Conf. on Electrical Contacts*, 2002, pp. 86 – 94.

[13] C. C. Hwang, J. J. Chang, and Y. H. Jiang, "Analysis of electromagnetic and thermal fields for a bus duct system," *Electric Power Systems Research*, vol. 45, pp. 39-45, 1998.

[14] Yu. A. Fominykh, Yu. A. Sokovishin, V. N. Osotov, D. S. Maslennikov, A. G. Konstantinov, M. E. Parylis, and A. M. Greditor, "Temperature distribution over the surface of rectangular busbars in electrical apparatus," *Elektrichestvo*, vol. 4, pp. 53-56, 1992.

[15] I. A. Metwally, "Thermal and magnetic analyses of gas-insulated lines," *Electric Power Systems Research*, vol. 79, pp. 1255-1262, 2009.

[16] M. D. Budinich, and R. E. Trahan, "Dynamic analysis of substation busbar structures," *Electric Power Systems Research*, vol. 42, pp. 47-53, 1997.

[17] A. F. Schneider, D. Richard, and O. Charette, "Impact of amperage creep on potroom busbars and electrical insulation: Thermal-electrical aspects," in *Light Metals - TMS 2011 Annu. Meeting and Exhibition,* San Diego, 2011, pp. 525-530.

[18] M. P. Paisios, C. G. Karagiannopoulos, and P. D. Bourkas, "Model for temperature estimation of dc-contactors with double-break main contacts," *Simulation Modelling Practice and Theory*, vol. 15, pp. 503 – 512, 2007.

**Adrian Pleşca** was born in Iasi, Romania, on April 16, 1972. He graduated from the Gheorghe Asachi Technical University of Iaşi and he received the PhD degree in Electrical Engineering in 2001. His employment experience included the Gheorghe Asachi Technical University of Iasi, Power Engineering Department. His special fields of interest included electrical apparatus, special equipment for power semiconductor devices protection and 3D modelling and simulation of the electrical apparatus. Dr. Pleşca received Golden and Silver Medals at World Exhibition of Invention, Research and Industrial Innovation, Brussels, Belgium, EUREKA, 2001, 2004, Special Prize awarded by National Research Council of Thailand for Fundamental Research at The First International Invention's Day Convention, Bangkok, Thailand 2008, Gold Medal at 4th International Warsaw Invention Show 2010, Diploma and Genius Medal at 2nd International Invention Exhibition, Ljubljana, 2010 and Gold Prize at Seoul International Invention Fair, Korea 2011.